A Study on the Prediction of the Optimum Performance of a Small-Scale Desalination System Using Solar Heat Energy

Yong-Joon Jun [1] (ID)**, Young-Hak Song [2] and Kyung-Soon Park [3,*]** (ID)

[1] Department of Architectural Engineering, Dong-Eui University, Busan 47340, Korea;
     solauspresident@gmail.com
[2] Department of Architectural Engineering, ERI, Gyeongsang National University, Jinju 52828, Korea;
     songyh@gnu.ac.kr
[3] Architectural Engineering Major, Division of Urban, Architecture and Civil Engineering,
     Dong-Eui University, Busan 47340, Korea
*   Correspondence: pks2180@deu.ac.kr; Tel.: +82-51-890-1986

Abstract: Although water is an essential element for the survival of all humankind, there are, however, still areas where water is not sufficiently supplied. It is a reality today that supplying energy for producing clean water is also difficult in such areas. This study develops a fresh water generator using solar heat, which is a clean energy source, and a small-scale desalination system which can be configured in parallel so that it can cope with various changes in the water supply situation. In addition, this study has developed a simulation program capable of estimating the optimum installation angle of a solar collector in such a way as to be suitable for the period of water demand, as well as the environment of the installation area, by allowing for the fact that it is difficult to change the installation angle or conditions after the installation of a fixed solar collector. In order to carry out these issues, this study has set up the experimental apparatus of a small-scale desalination system and obtained data on the amounts of fresh water generation depending on solar heat storage temperatures through empirical experiments. By applying the data in the simulation program, this study proposed the optimum installation angle for the necessary conditions.

1. Introduction

Water is one of the most widely used resources on the Earth. However, sufficient water supply is still not fully achieved in some areas of the world. Some countries in the Middle East use multi-stage flash distillation that utilizes oil, natural resources, or reverse osmosis, which utilizes electrical energy in order to desalinate seawater [1]. However, the desalination methods require massive amounts of fossil fuels or electrical energy. These accelerate greenhouse gas emissions and climate change, which in return may further aggravate the water shortage phenomena [2].

Solar thermal energy is the most stable heat source among the new and renewable energy sources. If seawater is evaporated by efficiently utilizing the enormous amount of solar thermal energy falling on the Earth and the seawater on the sea floor whose temperature is lower than the dew-point temperature of water vapor is used as condensate cooling water, it will be possible to embody a desalination system capable of producing clean water without using fossil fuels. Therefore, the research promptly commenced on these proposals.

Dai and Zhang [3] performed research on the relationship between the flow rate of incoming seawater and the amount of fresh water generation in the solar thermal seawater desalination system

which sprays seawater heated by the solar thermal collector in the form of mist, thereby allowing air to pass through it and increasing the absolute humidity of the air and, thus, generates fresh water when the air comes in contact with the flow path where cold seawater flows. Parekh et al. [1] conducted research on the technique of generating fresh water by heating seawater by means of solar heat. Qiblawey and Banat [4] carried out research on the theoretical principle and economic efficiency evaluation of the multi-stage flash seawater desalination system which heats seawater in several stages by means of solar heat. Bahnemann [5] performed research on the technique of purifying polluted water by using solar heat directly as a photocatalyst. Li et al. [6] carried out research on the cost and performance of various solar desalination systems.

Solar heat collection used in solar desalination system is most influenced by the type of solar collector. Martinopoulos et al. [7] performed research on the performance characteristics of solar collectors according to the flow rate of a flat type solar collector. Horta et al. [8] carried out research on the performance characteristics of solar collectors focused on desalination cost.

Collectable solar thermal energy resources may differ according to the area where a desalination system will be installed because there are latitudinal and environmental diversities among different areas. Therefore, in order to estimate the amount of fresh water generated using solar heat, it is necessary to gauge the amounts of solar thermal energy by the installation location for the system and the amount of energy collection according to the installation angle of the solar thermal collector used to collect solar heat.

Yoon et al. [9] developed an algorithm to calculate the cloud cover for estimating the solar thermal energy which passes through the atmosphere and reaches the ground surface. Khorasanizadeh et al. [10] proposed a diffuse solar radiation estimation model for Tabass, Iran and calculated the solar radiation on inclined surfaces based on each installation angle of a solar thermal collector. Corredor [11] calculated the solar radiation on inclined surfaces based on each installation angle of a solar thermal collector in seven areas of Colombia and then compared each calculation result with the physically-measured value corresponding to it. Al-Rawahi et al. [12] proposed a formula for calculating hourly solar radiation on inclined surfaces. Whereas, in the existing studies, it is possible to estimate diffuse and direct solar radiation separately only when the solar constant and the rate of solar radiation energy passing through the atmosphere is fully recognized, Zhang et al. [13] presented a solar radiation estimation formula containing the weather observation variables for the dry-bulb temperature, the relative humidity, the sunshine duration, and the cloud cover. Kim et al. [14] derived a correlation equation for the total solar radiation passing through the atmosphere and reaching horizontal surfaces by means of the weather observation variables exclusively for the dry-bulb temperature, the relative humidity, and the sunshine duration in order to make up for the inaccuracy of the cloud cover information based on the insufficient observation points. Cho et al. [15] measured solar radiation on inclined surfaces according to each tilt angle of a solar thermal collector in Daejeon, Korea, then subsequently compared each measurement result with the calculation result of the proposed solar radiation estimation formula for each corresponding case.

Yuan et al. [16] constructed a solar desalination system based on the humidification-dehumidification process and experimented with water generation. Al-Kharabsheh and Yogi [17] fabricated a water desalination system using low-grade solar heat and compared the study results with the theoretically-predicted values. Orfi et al. [18] carried out the experiments and theoretical study of a humidification-dehumidification sea water desalination system using solar energy. The above-mentioned previous studies provide this study with the idea of having the solar desalination system installed and comparing the experimental results with the theoretical ones. However, the previous studies have disadvantages in that the condenser and the evaporator are separated. Consequently, they cannot be modularized, and there is no consideration of the angle of the solar collector and the amount of the solar energy collection.

The purpose of this study is to make it easy to modify the capacity of the desalination system to meet demand. Therefore, this study devised a fresh water generator having a special structure that evaporates and condenses simultaneously.
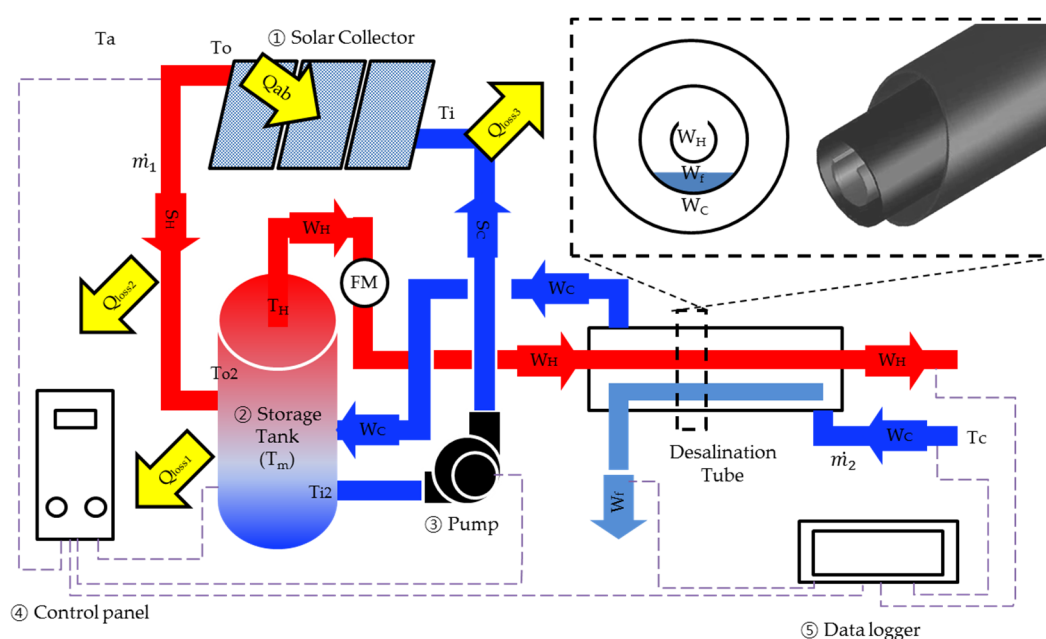
By devising a pipe-structured seawater desalination system capable of the parallel unit configuration, this study seeks to develop a performance prediction simulation program based on the optimum installation location of the system and the installation conditions for a solar thermal collection system. Due to these findings, this study set up an experimental apparatus, measured the amounts of fresh water generation according to the temperatures of solar-heated water, then derived the correlation equations relating thereto.

After creating a solar thermal collection simulation program based on the installation latitude of the desalination system and the installation angle of the solar thermal collector, this study calculates the heating temperatures of seawater then subsequently performs numerical analysis of the amounts of fresh water generation accordingly. Furthermore, to practically cope with the water demand, which changes each month, this study proposes the installation angle of a solar thermal collector at which the seasonal amounts of fresh water generation are greatest.

2. System Configuration

2.1. Experimental Apparatus

The experimental apparatus used in this study consists of the following: a ① solar collector, a desalination system, a ② pump for driving the heat transfer medium, a ② solar storage tank, a ⓕⓜ flow control meters for controlling the flow rate, a ④ control panel for pump efficiency and automatic control, a ⑤ data logger for collecting various measurement data, a carbon filter for water improvement, and the schematic diagram is shown in Figure 1. As shown in Figure 1, the freshwater generating pipe is composed of three concentric pipes. In the center, the heated sea water (W_H) flows and generates vapors in the second pipe. At this time, the cold sea water flows between the second and third pipes and cools down the surface temperature of the second pipe. Thus, the condensed freshwater (W_f) is collected in the second pipe and collected into the measuring device. Next, the cooling water (W_C) is stored in the storage tank and heated by the solar collector during the daytime. Heated sea water flows into the freshwater generator to generate water vapor in the evening. Figure 2 shows the installed pictures of the experimental equipment.

Figure 1. Schematic diagram of solar desalination system in this study.

Figure 2. Pictures of the experimental equipment.

Existing desalination plants have presented a difficulty in making them modular or small-scale. To tackle this challenge, the structure of this seawater desalination system has been devised on the belief that if fresh water generation units made each in the form of a pipe are connected in parallel, it is possible to control the capacity of the system in such a way as to meet with the water demand. Table 1 shows detailed specifications of the experimental apparatus. The experimental apparatus is divided up into the heat storage part and the fresh water generation part. The inflow of cooling water is suspended for a period between 7:00 a.m. until 7:00 p.m. ($m_2 = 0$). The pump only operates when the temperature of the solar thermal collector is higher than the temperature of the heat storage tank ($T_{o2} < T_o$), and the water is heated by the solar thermal collector and then stored again in the solar thermal collector. Specifications of experimental equipment and instruments are shown in Tables 1 and 2.

For coding simulation program in this study, the energy equations for the state quantity at each part of the experimental apparatus are as follows:

$$Q_{ab,n} = m_1 C_h (T_{o,n} - T_{i,n}) \tag{1}$$

$$\frac{T_a - T_o}{\left(\frac{\ln\left(\frac{r_2}{r_1}\right)}{2\pi k_1 L} + \frac{1}{2\pi r_2 h_2 L} \right)} = m_1 C_h (T_{o2,n} - T_{o,n}) \tag{2}$$

$$Q_{loss1,2} = \frac{\left(\frac{\pi d^2}{4} + \pi d H \right)}{\left(\frac{1}{h_1} + \frac{g_1}{k_2} \right)} \times (T_{m,n} - T_a) \tag{3}$$

$$m_1 C_h (T_{m,n-1} - T_{o2,n}) \times x_{day} + V C_w (T_{m,n} - T_{m,n-1}) + m_2 C_w (T_H - T_C) \times \left(1 - x_{day} \right) + Q_{loss} = 0$$
$$\left(\begin{array}{l} x_{day} = 1, \ AM7 \sim PM7 \\ x_{day} = 0, \ PM7 \sim AM7 \end{array} \right) \tag{4}$$

In this case, 100 mm was applied as the insulation thickness of tank, g_1, of the lagging for the solar heat storage tank, and the convective heat transfer coefficients, h_1 and h_2, are calculated with the equations given below [19]. In addition, it was discovered that any friction loss in the piping does not greatly affect the calculation results even if it is assumed that the temperature in the piping

is decreased linearly by heat loss. Thus, the temperature value at the outlet was used to reflect the greatest heat loss.

Table 1. Specifications of solar desalination system in this study.

Classification	Details	
Place of experiment	Busan (Latitude 35.10°)	
Period of experiment	11 April 2016–6 May 2016	
Hours of solar heat storage	7:00 a.m.–7:00 p.m. (12 h)	
Hours of desalination	7:00 p.m.–7:00 a.m. (12 h)	
Installation angle	45°	
Operation conditions	Amount of incoming cooling water: 0.8 L/min Temperature of hot water (seawater): 70 °C, 60 °C, 50 °C, 40 °C Temperature of cooling water (seawater): 15 °C	
Solar collector	Type	Flat type
	Size	1180 × 2400 × 92 mm
	Quantities	3 panel
	Glass	Low-iron glass (transmit rate: 91.7%) with 4 mm thickness
	Absorber	Titanium coated copper plate (emission rate : $4 \pm 1\%$, Absorption rate : $95 \pm 1\%$) with 0.2 mm thickness
	Insulation	Glass wool 0.040 W/mK with 40 mm thickness (bottom) PE form 0.035 W/mK with 15 mm thickness (side)
	Pipe	φ22.2 mm × 2 EA and φ8 mm × 10 EA
Solar storage tank	300 L (φ650 × 900H, 100 mm glass wool insulation)	
Etc.	Pump (7 m, 50 LPM, inline pump), 15 mm HDPE (High Density Polyethylene) pipe with 40 mm insulation	

Table 2. Technical specification of instrumentations used in this study.

Instrumentation/Type	Range	Accuracy
Data logger (20 Channel)	−100 to 1370 °C	±0.8 °C
Temperature sensor/K-type thermocouple	0−200 °C	±0.75%
Flow control valve Floating flowmeter	0.03−30 m³/h	±2%
Scale/electronic	0−2000 g	±0.2%

The performance of systematic solar desalination system like the one used in this study is highly influenced by solar collector types. In order to heat sea water to a high temperature, it is advantageous to use a vacuum tube solar collector, but this study was carried out near the sea, so it was necessary to pay attention to cost and durability. Therefore, the experimental system on this study was performed with flat-type solar collectors.

$$h = 3.95 + 5.8v \ \left(\text{W/m}^2\text{K} \right) \ (v \leq 5 \ \text{m/s}) \tag{5}$$

$$\frac{T_{i2} - T_a}{\left(\frac{\ln(r_2/r_1)}{2\pi k L} + \frac{1}{2\pi r_1 h_2 L} \right)} = m_1 C_h (T_{i2} - T_i) \tag{6}$$

The solar heat storage part stops operating for a period between 7:00 p.m. until 7:00 a.m. on the following day, whereas only the fresh water generation part operates for the same period. During this period, the cooling water whose flow rate is m_2 = 0.8 LPM flows directly into the fresh water generator and functions as such, after which it flows into the heat storage tank. The same amount of seawater is then heated to a high temperature in the top part of the heat storage tank as the amount of the cooling water that has flowed into the fresh water generator and then flash-evaporates, thereby generating water vapor, after which it is discharged in the sea. By operating the solar thermal desalination

system for 26 days from 11 April 2016 through 6 May 2016, this study measured the hourly amounts of fresh water generation according to the temperature conditions of hot water flowing from the heat storage tank into the fresh water generator. Experiments were conducted using real seawater supplied by the National Institute of Fisheries Science. The supply water was the seawater of a constant temperature (15 °C) pretreated in the experimental laboratory. The experiments were performed under the respective four conditions of the temperature from the seawater in the heat storage tank being 70 °C, 60 °C, 50 °C, and 40 °C. In order to obtain more accurate temperature values, a limiter was installed in each real experiment to stop the operation of the pump whenever the temperature of the heat storage tank becomes the temperature required for the experiment.
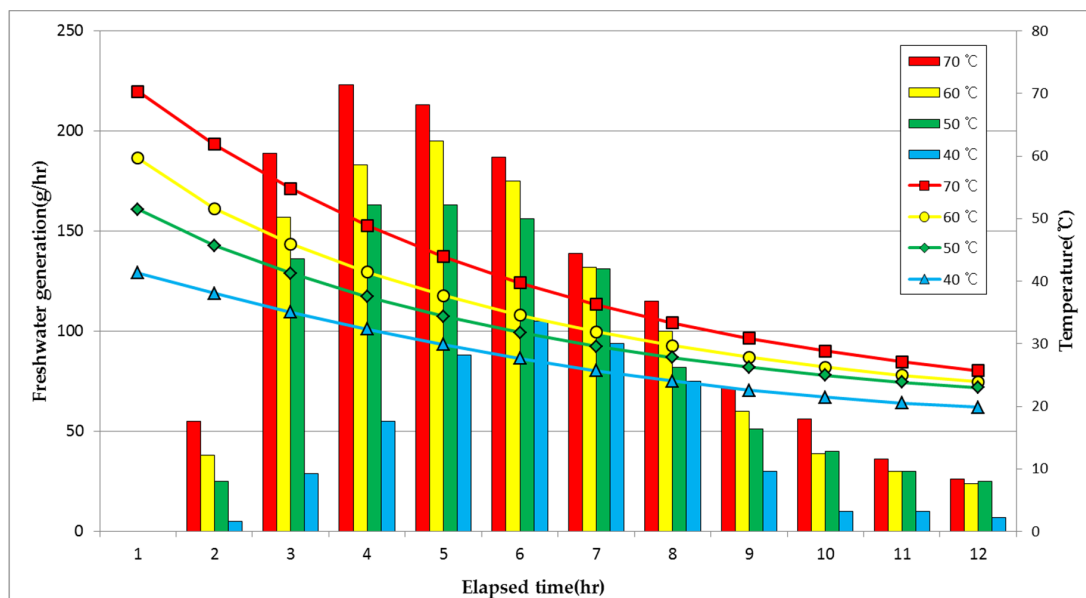
2.2. Experimental Results

The hourly temperature changes of the heat storage tank and accumulated sunshine hours are shown in Figure 3. The heat storage control starts to operate at 7:00 a.m., and it can be seen that the temperature of the heat storage tank begins to rise from the time when the temperature of the solar thermal collector becomes higher than the temperature of the heat storage tank. The highest temperature that was stored in the heat storage tank under the relevant installation angle conditions in April was approximately 74 °C, and the heat was no longer stored after 4:00 p.m. One can notice that the temperature shows a trend falls slightly due to the loss of heat outside at this time. Although the temperature range after the heat storage was between 45–75 °C according to the day's weather conditions, it was confirmed that the temperature range was located between 16–17 °C after the water heated by the fresh water generator was used for a period from 7:00 p.m. until 7:00 a.m. on the following day. This is considered to be due to the fact that the temperature of the tap water being supplied was almost constantly 15 °C and that almost all the hot water was used until the following day while staying in thermal equilibrium with the seawater being supplied. The sunshine hours of the temperature sampling date were used as weather data and averaged over time. Although the hourly insolation weather data shows a decrease after 6:00 p.m., the temperature of the solar thermal storage tank starts to decrease after 5:00 p.m. This is due to the difference between the positions of the meteorological measurement site and the location of the experimental equipment in this study. However, the overall pattern shows a similar tendency to the temperature according to passing time.

Figure 3. Temperature distribution of the heat storage tank and accumulated sunshine hours (11 April–6 May, 7:00 a.m.–7:00 p.m.).

Figure 4 shows a comparison between the hourly temperature changes in the heat storage tank according to the seawater temperature conditions and the amount of fresh water generation. There is, however, no fresh water generated for one hour after the system starts working, which is thought to be due to the fact that it takes some time for fresh water to start falling and be collected after the formation of water drops at the dew-point temperature during the evaporation of seawater. After the system started to operate, the amount of fresh water generation began to increase, and it was discovered that the amount of fresh water generation per hour was the highest during the fourth or fifth hour interval.

Figure 4. Amount of fresh water generation and temperature distribution by storage temperature.

However, the amount of fresh water generation starts to decrease after the passage of 4–5 h as a result of the temperature from the heat storage tank dropping steadily due to the inflow of cold water serving as cooling water. In the total amount of fresh water generated for 12 h, there was a performance difference of approximately 10% per 10 °C between 50 °C and 70 °C. When the temperature of the heat storage tank was at 40 °C, the greatest amount of fresh water generation was discovered during the sixth hour interval, and it was also confirmed that the total amount of fresh water generation fell below 50% at 50 °C. This is considered to be due to the fact that the amount of water evaporating decreases conspicuously under the temperature condition of 40 °C, thus causing some time to be required for fresh water to start falling from the surface of the cooling pipe.

Figure 5 is a graph displaying the amount of fresh water generated during each relevant hourly interval according to the temperature of the heat storage tank changing on an hourly basis in each process.
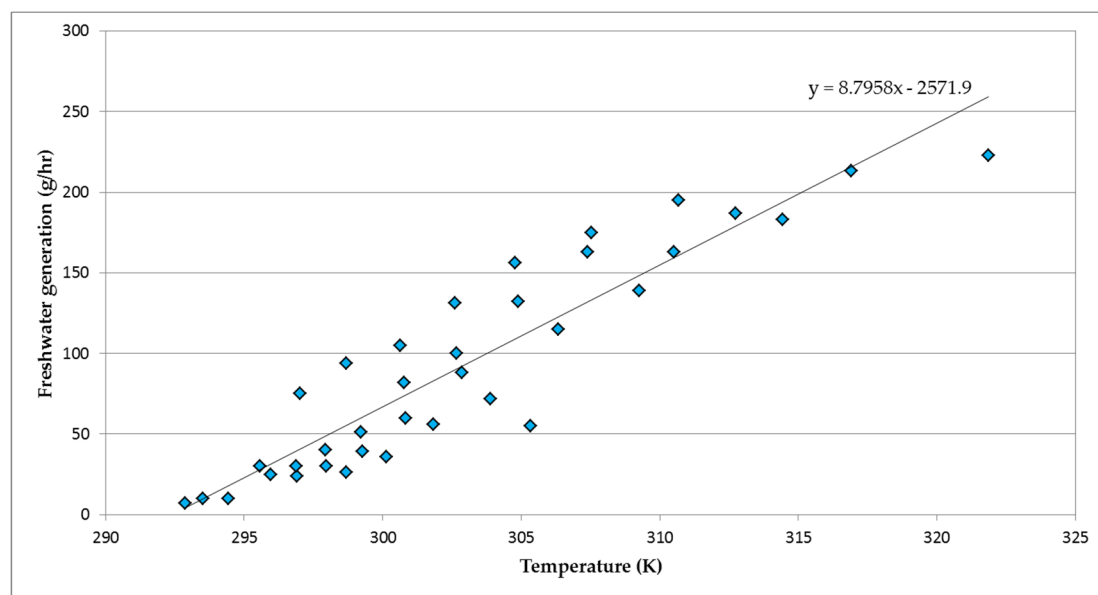
As described above, it takes approximately five hours for effective fresh water to be generated in a normal state after the equipment starts operating. Thus, the temperature of the heat storage tank and the amount of fresh water generation during the relevant hour interval after the passage of five hours since the startup of the system operation show a linear relationship between them on the whole. This relationship can be predicted by a means of the following empirical formula:

$$y = 8.7958x - 2571.9 \ (\text{g/h}) \tag{7}$$

where,

y: freshwater generation (g/h)
x: temperature of storage tank (K)

Figure 5. The amount of fresh water generation by the hourly temperature of the heat storage tank.

3. Simulation

3.1. Solar Radiation Data

This study used the respective mean values of the hourly dry-bulb temperatures, relative humidity, wind speeds, and the durations of sunshine between 2010 and 2016 in each of the seven areas across the country (Gwangju, Daegu, Daejeon, Busan, Seoul, Ulsan, and Jeju), which were provided by the Korea Meteorological Administration. In the case of each area where the measured values of the total solar radiation on horizontal surfaces were omitted, the comparison of the simulation results and the measured values were excluded. The latitude values of the weather observation points in the relevant area were used to represent their latitudes in Table 3.

Table 3. Latitudes of representative areas [14].

Area	Gwangju	Daegu	Daejeon	Busan	Seoul	Ulsan	Jeju
Latitude (°)	35.17	35.83	36.37	35.10	37.57	35.58	33.51

3.2. Estimation of the Total Solar Radiation on Horizontal Surfaces

3.2.1. Formula for Estimating the Total Solar Radiation on Horizontal Surfaces

The sunlight reaching the surface of the Earth consists of direct and diffuse components. However, in the case of a light collection system which obtains high-temperature energy by collecting sunlight over a wide area into one place, most accept the total solar radiation without dividing it into its direct and diffuse components. Therefore, just to confirm the solar heat gain on the tilted angle this study used the total solar radiation without dividing it into its direct and diffuse components. Total solar radiation on horizontal surfaces is required initially for estimating the optimum installation angle of a solar thermal collector. Since there are only 15 areas across the country for measuring the total solar radiation on horizontal surfaces, widening the simulated estimation range requires a technique for estimating the total solar radiation on horizontal surfaces based on the weather observation data on temperatures, humidity, wind speeds, sunshine durations, and cloud cover. Pointing out the insufficiency of Korea's domestic cloud cover data, Kim et al. and Park et al. presented respective

equations for estimating the total solar radiation on horizontal surfaces based on the temperatures, humidity, wind speeds, and sunshine durations in the relevant areas [14,20]:

$$I_1 = I_0 \sin(\alpha)\{\beta_0 + \beta_1(T_{db,n} - T_{db,n-3}) + \beta_2 RH + \beta_3 V_w + \beta_4 t_{ds}\}$$
$$\beta_0 = 0.44645, \; \beta_1 = -0.0147, \; \beta_2 = -0.327, \; \beta_3 = 0.00362, \; \beta_4 = 0.391$$

(8)

3.2.2. Comparison with the Measured Values of the Total Solar Radiation on Horizontal Surfaces

Table 4 shows a comparison between the measured values of total solar radiation on horizontal surfaces in Busan. Table 4 also reveals the amounts of total horizontal solar radiation expected based on the weather data from 2016 in order to ascertain the reliability of the calculation results of the total solar radiation on horizontal surfaces. The annual average ratio of the simulation results to the measured values of the total solar radiation on horizontal surfaces in each area is as shown in the following Table 5. The simulation results of the total solar radiation on horizontal surfaces in low-latitude areas such as Busan and Ulsan are close to the measured values overall. It can also be seen that errors are greater between the simulation results and the measured values in more northern areas, such as Seoul and Daejeon. Although it is highly necessary to consider the reduction of solar radiation or the occurrence of measurement errors due to air pollution when it comes to the measured values obtained mainly in metropolitan cities and provinces in particular, it is true that data is still insufficient today.

Table 4. Comparison of the measured values of the total solar radiation with the simulation results (Busan, 2016).

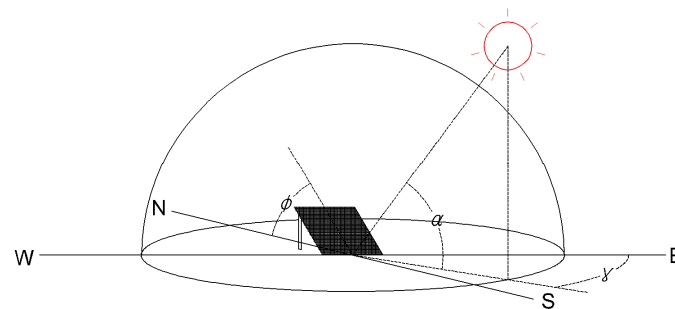| Month	Measured Value (A, MJ/m^2 day)	Simulation Result (B, MJ/m^2 day)	A/B
1	10.13	10.43	0.97
2	11.50	11.52	0.97
3	15.07	15.42	0.96
4	17.25	17.83	0.96
5	19.64	20.05	0.98
6	16.69	16.51	1.01
7	17.33	16.52	1.05
8	16.59	16.39	1.01
9	14.32	14.41	1.01
10	12.76	12.80	1.00
11	9.58	9.86	0.98
12	8.57	9.27	0.96
Average	14.12	14.25	0.99

Table 5. The annual average ratio of the results from the simulation to the measured values of the total solar radiation on horizontal surfaces.

Area	Gwangju	Daegu	Daejeon	Busan	Seoul	Ulsan	Jeju
A/B	1.04	0.89	1.13	0.99	0.89	0.96	1.07

3.2.3. Solar Radiation on Inclined Surfaces

The sun light strikes the inclined surfaces of the solar thermal collector as shown in Figure 6. The collected radiation energy is calculated with the equation below:

$$I_2 = \frac{I_1 \sin(\gamma + 90) \sin(\alpha + \varphi)}{\sin(\alpha)}$$

(9)

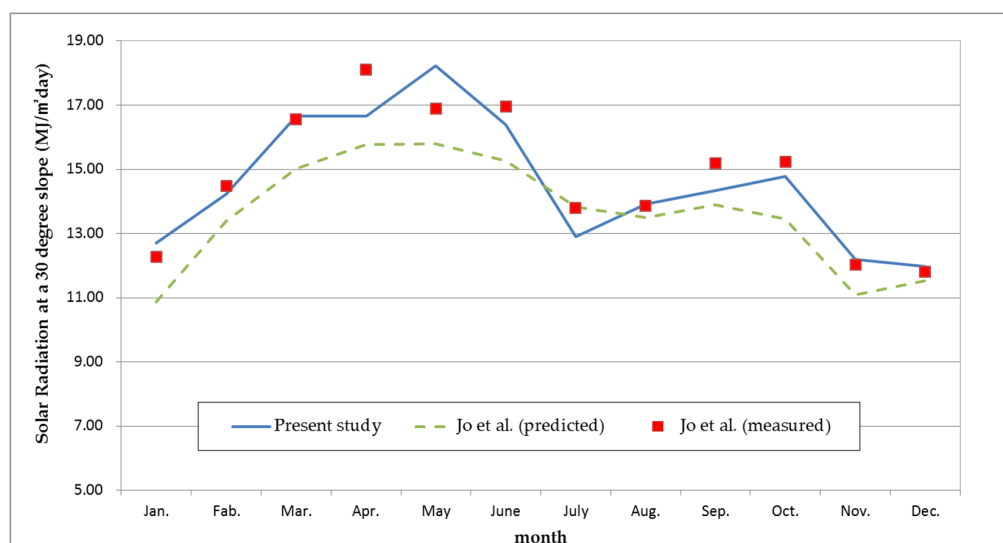**Figure 6.** Radiation by solar altitude and azimuth.

3.2.4. Solar Radiation on Inclined Surfaces and the Amount of Collected Heat

The solar radiation on inclined surfaces, the efficiency of heat collection, and the amount of collected solar heat were calculated based on a solar hot water system as mentioned in Table 6.

Table 6. Simulation conditions.

Parameter	Value/Type
Area	Daejeon
Installation angle	30°
Installation direction	Due South
Number of Solar collection sheets	3 EA
Solar collection area per sheet	2.83 m^2
Flow rate per sheet	0.02 kg/s
Hot water storage tank (L)	300

Jo et al. [21] and Basunia et al. [22] have divided the total solar radiation on horizontal surfaces into its direct and diffuse components and then compared the solar thermal energy striking inclined surfaces with the measured values. In this particular study, the total solar radiation was calculated without dividing it into its direct and diffuse components by taking the flat-plate solar collector into account, and as no real significant difference is noticed between the calculation results of this study and the simulation and the actual measurement data from previous studies in Figure 7, the reliability of using the total solar radiation data was confirmed.

Figure 7. Comparison of solar radiations at a 30° slope in the present study (MJ/m^2 day).

The annual average efficiency of the solar hot water system in Daejeon was calculated to be 51%, and the monthly average amount of collected solar heat was discovered to be 7.73 MJ/m². As there is no reliable actual measurement data on the solar hot water system, it is quite difficult to perform any quantitative comparison and secure its reliability. According to the resulting values of the test report of the solar collector model used in the simulation, if the solar radiation is 21 MJ, the amount of collected solar heat is 9.4 MJ (44.7% of the solar radiation). However, when the measured value of the solar radiation in May as shown in Table 7 is 19 MJ, the amount of collected solar heat is 9.71 MJ (51.1% of the solar radiation), thus showing an error of approximately 7% between them.

Table 7. Estimation of the daily average solar radiations and the amount of heat collected by the solar collector (30°, Daejeon).

Month	Daily Average Solar Radiation (MJ/ m² day) Jo et al. Predicted	Daily Average Solar Radiation (MJ/ m² day) Present Study	Average Efficiency (η)	Amount of Collected Heat (MJ/ m² day)
1	12.28	13.18	0.48	6.26
2	14.47	14.54	0.50	7.28
3	16.56	17.12	0.53	9.09
4	18.11	17.26	0.56	9.60
5	16.88	19.00	0.51	9.71
6	16.96	17.00	0.55	9.37
7	13.79	13.42	0.49	6.61
8	13.86	14.50	0.57	8.23
9	15.19	14.74	0.56	8.29
10	15.23	15.07	0.50	7.60
11	12.02	12.55	0.44	5.59
12	11.81	12.43	0.41	5.10
Average	14.76	15.07	0.51	7.73

3.3. Calculation of the Amount of Fresh Water Generation

3.3.1. Heat Collecting Efficiency of the Solar Collector

The heat collecting efficiency of the solar collector is calculated with the equation given below [23]:

$$\eta = \frac{Q_{ab}}{I_2} \tag{10}$$

In this case, it is possible to estimate the heat collecting efficiency of the solar collector using a quadratic expression formed with its inlet and outlet temperatures and the solar radiation striking it [23].

$$\eta = a_0 + a_1 \left(\frac{T_b - T_a}{I_2} \right) + a_2 \left(\frac{(T_b - T_a)^2}{I_2} \right) \tag{11}$$
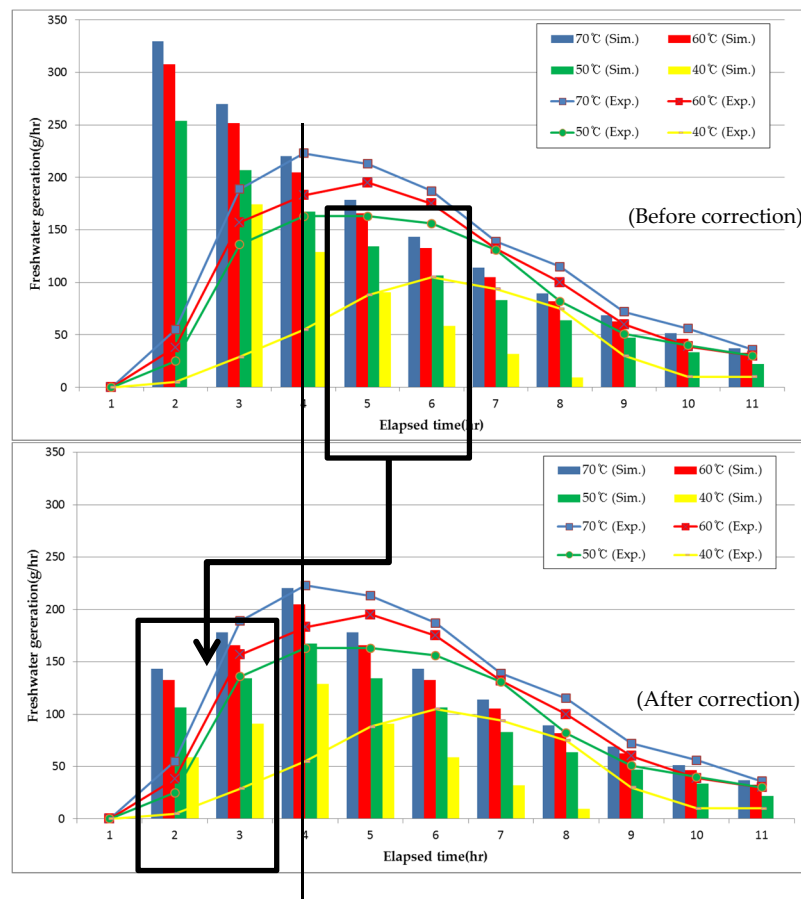
$$T_b = \frac{T_o - T_i}{2} \tag{12}$$

Having flowed out of the outlet after being heated in the solar collector, the heat transfer medium carries out a heat exchange with the bottom part (tap water) of the heat storage tank. Thus, by assuming that the heat exchange temperature is equal to the weighted average value between its temperature and the tap water temperature during the relevant hourly interval, the temperature of the heat transfer medium at the inlet for the next hour interval was estimated, and the coefficients used in the equation are as shown in Table 8.

Table 8. Efficiency formula of the KS (Korean Industrial Standards) standard for collector types.

Item	Flat-Plate Type	Single Vacuum Tube	Reflector Double Vacuum Tube
a_0	0.771 ± 0.058	0.721 ± 0.007	0.664 ± 0.078
a_1	5.091 ± 0.611	1.483 ± 0.758	2.829 ± 1.996
a_2	0.0048 ± 0.0071	0.0055 ± 0.0047	-0.0005 ± 0.0126

3.3.2. Calculation and Verification of the Amount of Fresh Water Generation

It is possible to calculate the amount of fresh water generation per hour during the operation of the fresh water generation system using the empirical formula and the hourly temperature values of the heat storage tank calculated with the energy equilibrium equations. A comparison between the experimental conditions and the simulation results for the same period is as shown in Figure 8. As described above, the simulation result value based on the temperature of the heat storage tank is greater than the actually measured values during the four hours for which sufficient energy is supplied to the system after the passage of four hours from the startup of the system operation. It can also be noticed that after the passage of four hours during which the system reaches its normal state, a simulation result similar to the actually measured value is obtained.

Figure 8. Amounts of fresh water generation according to the heat storage temperatures and times.

The amount of fresh water generation on the left and right side of the four hour point, which shows a maximum value, is similar in pattern. Simulation results of fresh water generation at two and three hours are replaced with those at five and six hours. Therefore, the difference rate between the experimental and simulation data of fresh water during the day is as shown in Table 9.
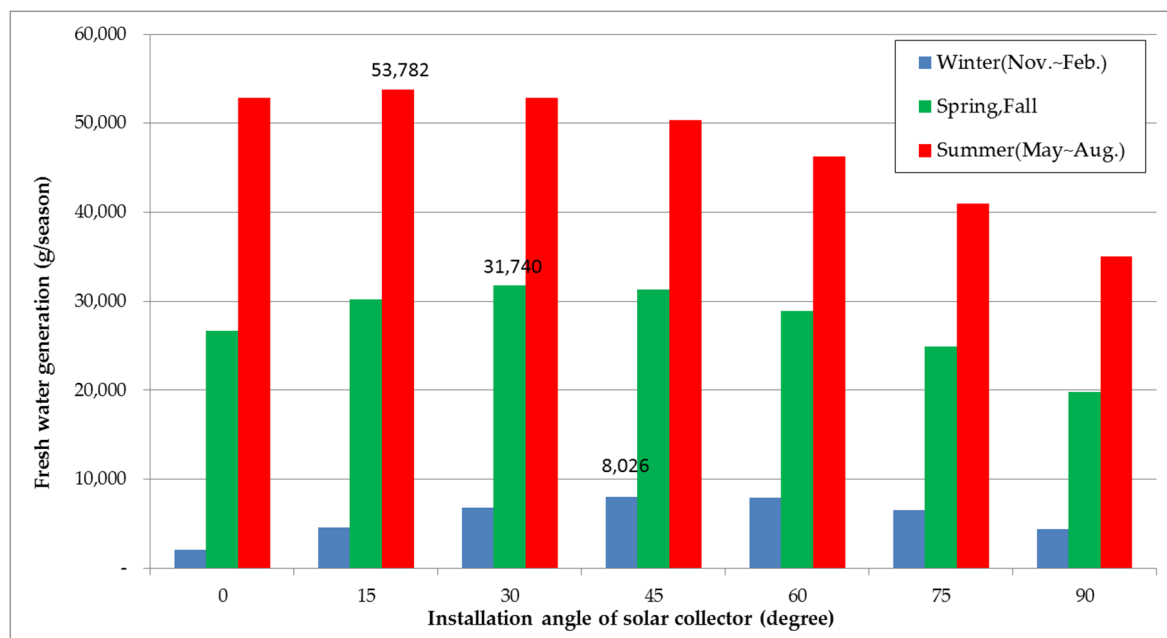
Table 9. Difference between the experimental and simulation data when the time difference is corrected.

Temperature	70 °C	60 °C	50 °C	40 °C
Difference Rate	95.26%	101.98%	91.92%	93.53%

Experimental results show the same tendency as the quadratic function curve with the maximum value of four hours, which is the peak value of fresh water generation. The freshwater discharge in the experiment is not consistent with the complete quadratic curve since the freshwater is generated and caught in the system and the time delay exists since fresh water was not collected in the experiment until the system was supplied with heat for a few hours. On the other hand, fresh water was generated in the simulation because the amount of fresh water generation was a function of temperature only. In order to compensate for this, we corrected the error by using the data for five and six hours instead of data for two and three hours. As a result, the difference of the fresh water generation during the day was about 6% at a maximum.

3.4. Comparison of the Amount of Fresh Water Generation According to the Installation Angle of the Solar Collector

The results from estimating the amounts of fresh water generation according to the installation angle of the solar thermal collector in Busan are as shown in Table 10. It was discovered that the greatest annual amount of fresh water was generated at an angle of 30°, and the distribution of the seasonal amounts of fresh water generation is as shown in Figure 9. Due to the monthly changes in the solar altitude angle, the largest seasonal amount of fresh water generation was shown by an installation angle of 45° in winter, 30° in spring and fall, and 15 degrees in summer. This can be confirmed to show significant results for the installation angle suitable for each season that needs water.

Figure 9. Freshwater generation by season according to installation angle of the solar collector.

Table 10. Monthly fresh water generation by the installation angle of the solar collector (g/day).

Month	0°	15°	30°	45°	60°	75°	90°
1	34	78	111	127	126	109	80
2	58	96	119	127	119	98	66
3	150	185	199	194	172	136	91
4	256	275	275	258	227	182	128
5	368	377	367	342	304	254	196
6	371	374	363	341	308	267	221
7	438	443	433	413	380	339	292
8	483	495	490	471	440	399	349
9	396	422	430	421	398	362	315
10	291	337	362	365	352	322	278
11	133	192	228	244	240	219	182
12	40	88	124	142	144	128	99
Total (g/year)	92,200	102,637	106,885	105,150	98,011	85,911	70,185

4. Conclusions

In order to make it possible to supply fresh water to small island areas or mountainous areas which require water, this study designed and constructed a system capable of generating fresh water by means of solar thermal energy, a clean energy source, measured hourly amounts of fresh water generation according to the heat storage temperature, designed a program for estimating the amount of fresh water generation according to the installation latitude and angle of the solar thermal collector on the basis of the measured data and, finally, derived the optimum installation conditions to meet the needs of the fresh water consumers.

(1) The actual amount of fresh water generation was discovered to be proportional to the temperature of solar heat storage during the daytime. The hourly solar heat storage temperature, as well as the hourly amount of fresh water generation, was also discovered to be linearly proportional to each other after the system reached its thermal normal state after the startup of its operation.

(2) This study created a program for estimating the solar radiation on inclined surfaces which does not need any cloud cover information for the purpose of designing an estimation program for areas without any cloud cover information, which is required for existing solar heat tracking simulation algorithms. As a result of comparing the simulation results obtained using the program with the measured values, it was confirmed that they match each other quite well.

(3) Hourly amounts of fresh water generation were estimated by applying an empirical formula derived as an experimental result by calculating the heat storage temperature of the solar thermal collector through the created solar heat tracking simulation program and, accordingly, it was confirmed that the estimation results were very similar to the experimental results after the system reached its thermal normal state.

(4) The length of time required for the system to reach its thermal normal state was considered to be four hours by this study, and the estimation results were confirmed to show an error of approximately 10% in comparison with the experimental results except in the case where the temperature of the heat storage tank is 40 °C.

(5) According to the simulation results, the largest annual amount of fresh water generation at the latitude (35.10°) of Busan was discovered when the solar thermal collector was installed at an angle of 30°. The largest seasonal amount of fresh water was generated at an angle of 45° in winter, at an angle of 30° in spring and fall, and at an angle of 15° in summer. This is thought to be due to the diverse monthly solar altitude angles.

Author Contributions: All authors participated in the research, analysis and interpretation of the data, as well as the design and production of this article. All authors agree to be listed and approve the submitted and accepted versions of the publication.

Conflicts of Interest: The authors declare no conflict of interest.

Nomenclature

I_0	Solar constant (1367 W/m^2)
I_1	Total solar radiation on horizontal surfaces 9 W/m^2)
I_2	Solar radiation on inclined surfaces (W/m^2)
α	Solar altitude angel (°)
m_1	flow rate of heat medium (kg/s)
m_2	flow rate of sea water (kg/s)
T_a	Temperature of air (°C)
T_o	Temperature of inlet of solar collector (°C)
T_i	Temperature of outlet of solar collector (°C)
T_H	Temperature of Heated sea water (°C)
T_C	Temperature of Cold sea water (°C)
T_m	Temperature of water storage tank (°C)
T_{i2}	Temperature of inlet of storage tank (°C)
T_{o2}	Temperature of outlet of storage tank (°C)
h_1	heat transfer coefficient of sea water in storage tank (W/m^{2}K)
h_2	heat transfer coefficient of heat medium in pipe (W/m^{2}K)
$T_{db,n}$	Drybulb temperature at n time (°C)
RH	Relative humidity (%)
V_w	wind velocity (m/s)
t_{ds}	sunshine durations (h)
γ	Solar azimuth angle (°)
φ	Inclined angle of solar collector (°)
Q_{ab}	Collected solar energy (W)
Q_{loss}	Heat loss (W)
h	Convective heat transfer coefficient (W/m^{2}K)
r_1	Inner diameter of pipe (m)
r_2	Outer diameter of pipe (m)
k_1	Heat transfer coefficient of pipe (W/m·K)
k_2	Heat transfer coefficient of storage tank insulation (W/m·K)
L	Length of pipe (m)
d	Diameter of storage tank (m)
H	Height of storage tank (m)
C_h	Specific heat of heat medium (kJ/kg K)
C_w	Specific heat of sea water (kJ/kg K)
η	Efficiency of solar collector (%)

References

1. Parekh, S.; Farid, M.M.; Selman, J.R.; Al-Hallaj, S. Solar desalination with a humidification-dehumidification technique-acomprehensive technical review. *Desalination* **2004**, *160*, 167–186. [CrossRef]
2. Yang, H.K. Water Balance Change of Watershed by Climate Change. *J. Korean Geogr. Soc.* **2007**, *42*, 405–420.
3. Dai, Y.J.; Zhang, H.F. Experimental investigation of a solar desalination unit with humidification and dehumidification. *Desalination* **2000**, *130*, 169–175. [CrossRef]
4. Qiblawey, H.M.; Banat, F. Solar thermal desalication technologies. *Desalination* **2008**, *220*, 633–644. [CrossRef]
5. Bahnemann, D. Photocatalytic water treatment: Solar energy applications. *Sol. Energy* **2004**, *77*, 445–459. [CrossRef]
6. Li, C.; Goswami, Y.; Stefanakos, E. Solar assisted sea water desalination: A review. *Renew. Sustain. Energy Rev.* **2013**, *19*, 136–163. [CrossRef]

7.   Martinopoulos, G.; Ikonomopoulos, A.; Tsilingiridis, G. Initial evaluation of a phase change solar collector for desalination applications. *Desalination* **2016**, *399*, 165–170. [CrossRef]

8.   Horta, P.; Zaragoza, G.; Alarcón-Padilla, D.C. Assessment of the use of solar thermal collectors for desalination. *Desalination Water Treat.* **2015**, *55*, 2856–2867. [CrossRef]

9.   Yoon, K.; Yun, G.; Jeon, J.; Kim, K.S. Evaluation of hourly solar radiation on inclined surfaces at Seoul by Photographical Method. *Sol. Energy* **2014**, *100*, 203–216. [CrossRef]

10.   Khorasanizadeh, H.; Mohammadi, K.; Mostafaeipour, A. Establishing a diffuse solar radiation model for determining the optimum tilt angle of solar surfaces in Tabass. Iran. *Energy Convers. Manag.* **2014**, *78*, 805–814. [CrossRef]

11.   Corredor, L.M. Estimation of Solar Radiation Incident on Horizontal and Tilted Surfaces for 7 Colombian Zones. *Int. J. Eng. Res.* **2013**, *2*, 362–366.

12.   Al-Rawahi, N.Z.; Zurigat, Y.H.; Al-Azri, N.A. Prediction of hourly solar radiation on horizontal and inclined surfaces for Muscat/Oman. *J. Eng. Res.* **2011**, *8*, 19–31. [CrossRef]

13.   Zhang, Q.; Huang, J.; Lang, S. Development of typical year weather data for Chinese locations/Discussion. *ASHRAE Trans.* **2002**, *108*, 1063.

14.   Kim, H.Y.; Kim, J. Correlation to Predict Global Solar Insolation and Evaluation of that Correlation for Korea (I). *New Renew. Energy* **2016**, *10*, 30–35. [CrossRef]

15.   Cho, Y.; Kim, Y.; Chung, K.S. A study of Optimum Slope Angles of Fixed and Azimuth Tracking Solar Collectors by Region, Period and Year. In Proceedings of the SAREK Summer Annual Conference, Pyungchang, Korea, 23–25 June 2010.

16.   Yuan, G.; Wang, Z.; Li, H.; Li, X. Experimental study of a solar desalination system based on humidification-dehumidification process. *Desalination* **2011**, *277*, 92–98. [CrossRef]

17.   Al-Kharabsheh, S.; Yogi, D. Analysis of an innovative water desalination system using low-grade solar heat. *Desalination* **2003**, *156*, 323–332. [CrossRef]

18.   Orfi, J.; Laplante, M.; Marmouch, H.; Galanis, N.; Benhamou, B.; Nasrallah, S.B.; Nguyen, C.T. Experimental and theoretical study of a humidification-dehumidification water desalination system using solar energy. *Desalination* **2004**, *168*, 151–159. [CrossRef]

19.   Jürges, W. *Der Warmeubergang an Einer Ebenen Wand*, 2nd ed.; R. Oldenbourg: München, Germany, 1924.

20.   Park, S.M.; Kim, J. Correlation to Predict Global Solar Insolation and Evaluation of that Correlation for Korea (II). *New Renew. Energy* **2016**, *12*, 24–29. [CrossRef]

21.   Jo, D.K.; Yun, C.Y.; Kim, K.D.; Kang, Y.H. A study on the estimating solar radiation using hours of bright sunshine for the installation of photovoltaic system in Korea. *J. Korean Sol. Energy Soc.* **2011**, *31*, 72–79. [CrossRef]

22.   Basunia, M.A.; Yoshio, H.; Abe, T. Simulation of Solar Radiation Incident on Horizontal and Inclined Surfaces. *J. Eng. Res. TJER* **2012**, *9*, 27–35. [CrossRef]

23.   Kim, J.B.; Rhie, S.M.; Yoon, E.S.; Lee, J.K.; Joo, M.C.; Lee, D.W.; Kwak, H.Y.; Baek, N.C. Thermal Characteristics of Domestic Solar Collector for Low-Themperature Applications. *J. Korean Sol. Energy Soc.* **2007**, *27*, 155–160.